Journal of Photochemistry & Photobiology, B: Biology 229 (2022) 112415

Contents lists available at ScienceDirect

Journal of Photochemistry & Photobiology, B: Biology

journal homepage: www.elsevier.com/locate/jphotobiol

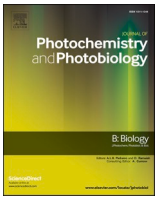

Biomimetic photooxidation of noscapine sensitized by a riboflavin derivative in water: The combined role of natural dyes and solar light in environmental remediation

Alice Pavanello [a], Debora Fabbri [b], Paola Calza [b], Debora Battiston [b], Miguel A. Miranda [a], M. Luisa Marin [a,*]

[a] Instituto de Tecnología Química, Universitat Politècnica de València-Consejo Superior de Investigaciones Científicas, Avda. de los Naranjos s/n, E-46022, Valencia, Spain
[b] Dipartimento di Chimica, Università di Torino, via P. Giuria 5, 10125 Torino, Italy

ARTICLE INFO

Keywords:
Drugs
Electron transfer
Excited states
Pollutants
Visible light

ABSTRACT

Noscapine (NSC) is a benzyl-isoquinoline alkaloid discovered in 1930 as an antitussive agent. Recently, NSC has also been reported to exhibit antitumor activity and, according to computational studies, it is able to attack the protease enzyme of Coronavirus (COVID-19) and thus could be used as antiviral for COVID-19 pandemic. Therefore, an increasing use of this drug could be envisaged in the coming years. NSC is readily metabolized with a half-life of 4.5 h giving rise to cotarnine, hydrocotarnine, and meconine, arising from the oxidative breaking of the C—C bond between isoquinoline and phthalide moieties. Because of its potentially increasing use, high concentrations of NSC but also its metabolites will be delivered in the environment and potentially affect natural ecosystems. Thus, the aim of this work is to investigate the degradation of NSC in the presence of naturally occurring photocatalysts. As a matter of fact, the present contribution has demonstrated that NSC can be efficiently degraded in the presence of a derivative of the natural organic dye Riboflavin (RFTA) upon exposure to visible light. Indeed, a detailed study of the mechanism involved in the photodegradation revealed the similarities between the biomimetic and the photocatalyzed processes. In fact, the main photoproducts of NSC were identified as cotarnine and opianic acid based on a careful UPLC-MS^2 analysis compared to the independently synthesized standards. The former is coincident with one of the main metabolites obtained in humans, whereas the latter is related to meconine, a second major metabolite of NSC. Photophysical experiments demonstrated that the observed oxidative cleavage is mediated mainly by singlet oxygen in a medium in which the lifetime of $^1O_2$ is long enough, or by electron transfer to the triplet excited state of RFTA if the photodegradation occurs in aqueous media, where the $^1O_2$ lifetime is very short.

1. Introduction

Noscapine (NSC) is a benzyl-isoquinoline alkaloid, present in concentrations of 2–8% as the second most abundant alkaloid in opium (Fig. 1) [1]. Noscapine was discovered in 1930 as an antitussive agent, probably because it depresses the citric acid-provoked cough [2–5]. More recently, in 1998, NSC was found to have also antitumor activity resulting from its binding to tubulin and inhibition of microtubule assembly. Thereafter, NSC has demonstrated activity against different types of tumors, both *in vitro* and *in vivo* [3,6–8]. Moreover, according to recent computational studies, NSC is able to attack the protease enzyme of Coronavirus (COVID-19) and thus could be used as antiviral for COVID-19 pandemic [9–12]. As a result, NSC is still considered a promising drug; in addition, contrary to other opium derivatives, it is nonaddictive and is not associated with sedative, euphoric or hypnotic side-effects. This is probably because, in contrast with the stronger, more addictive opioids, NSC does not bind to the μ-opioid receptor[13]. Furthermore, NSC does not act as an immunosuppressor [2,14]. Consequently, it can be anticipated an increasing use of NSC, which may imply a widespread release to the environment over the coming years. In the living organisms, detoxification of xenobiotics is achieved by means of a complex enzymatic machinery, which is responsible for a variety of

* Corresponding author.
E-mail address: marmarin@qim.upv.es (M.L. Marin).

https://doi.org/10.1016/j.jphotobiol.2022.112415
Received 13 September 2021; Received in revised form 15 February 2022; Accepted 21 February 2022
Available online 24 February 2022

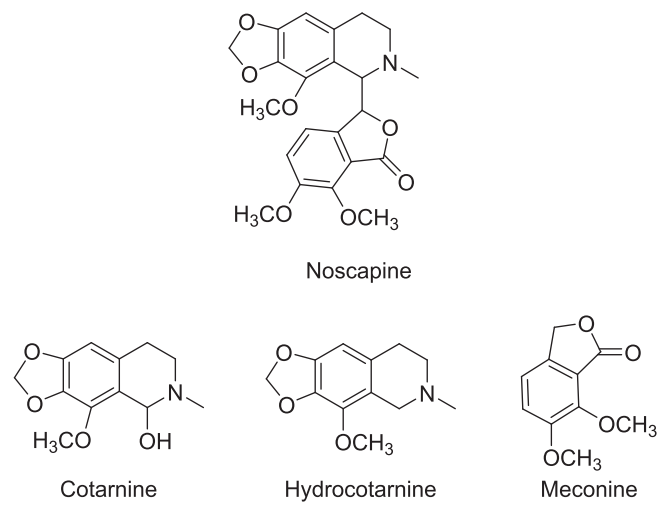

Fig. 1. Chemical structure of Noscapine (NSC), and its metabolites Cotarnine, Hydrocotarnine and Meconine.

metabolization pathways. In this context, several studies have been done to determine the pharmacokinetics of NSC, which is readily metabolized, leading to a relatively reduced bioavailability (around 30%), as a consequence of the first-pass loss. As a matter of fact, NSC is extensively biotransformed after oral administration (terminal half-life 4.5 h) [15], giving rise to three major metabolites (cotarnine, hydrocotarnine, and meconine), which result from the oxidative cleavage of the C—C bond linking the isoquinoline and phthalide moieties (Fig. 1) [16,17]. This natural biotransformation pattern seems inspiring to deal with the increasing amounts of NSC that could be delivered in the environment and potentially affect natural ecosystems.

Riboflavin (RF) (Fig. 2), also known as vitamin B2, is a natural organic product, present in fruits, vegetables and microorganisms, also found as an ingredient of the natural organic matter (NOM) in the aqueous systems. It absorbs visible light and as a result, it is known as an oxidative photocatalyst, acting not only from its excited states (electron transfer mechanism or Type I mechanism), but also indirectly upon generation of singlet oxygen (Type II mechanism) [18]. Thereafter, natural RF and also the more stable and commercially available acetylated riboflavin (RFTA) [19], have been proposed as non toxic photocatalysts for wastewater remediation [20–23]. More recently, RF has been covalently anchored to an inorganic support in order to prevent the formation of singlet oxygen and thus the photodegradation of RF. As a result, a more efficient photodegradation of contaminants has been achieved and the recyclability of the photocatalyst has been demonstrated [24].

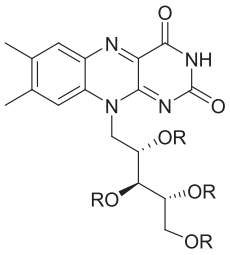

R	Name
-H	Riboflavin (RF)
-$COCH_3$	Acetylated Riboflavin (RFTA)

Fig. 2. Chemical structure of riboflavin (RF) and its acetylated derivative (RFTA).

Thus, this contribution addresses the overall abatement of NSC in the presence of dye RFTA, upon exposure to visible light. A detailed study of the mechanisms involved in the photodegradation reveals the similarities between the biomimetic and the photocatalyzed processes. These preliminary results point to the possibility of developing bio-inspired remediation processes based on the use of natural, non-toxic dyes operating through photocatalytic mechanisms similar to the *in vivo* biotransformation pathways, thus leading to degradation products with a low environmental impact.

2. Experimental

2.1. Chemicals

Noscapine, Riboflavin, and Rose Bengal were from TCI Chemicals and/or Merck Life Sciences SRL. Dimethylformamide (DMF) and acetonitrile were from Scharlau. Acetylation of RF was achieved as reported previously [25]. Cotarnine and Opianic acid were obtained from Noscapine, according the procedure reported in literature [26]. Water was Milli-Q grade. All the reagents were of analytical grade and used as received.

2.2. Photodegradation and Analytical Procedures

Irradiation of aqueous solutions of NSC (10 ppm) in the presence of RFTA (1 ppm) was performed in Pyrex vessels, using a 1500 W Xenon lamp and a 420 nm cut-off filter. Details of the procedure can be found elsewhere [27]. The progress of the photodegradation was followed by HPLC, using a reverse phase column and a UV–Vis detector, under the previously reported conditions [28]. The eluent was an aqueous solution of trifluoroacetic acid (TFA 0.1%*v*/v), brought at pH 9.6 with NaOH/acetonitrile (45/55, v/v). The detection wavelength was 225 nm for NSC and 460 nm for RFTA.

Separation and identification of the photoproducts were achieved by a UPLC-Waters system, provided with a C18 column, coupled to a QToF spectrometer. The mobile phase was composed of 0.1% aqueous formic acid solution (component A) and 0.1% formic acid in acetonitrile (component B). The column was equilibrated with A:B (70:30, *v*/v) as the mobile phase at a flow rate of 0.3 mL/min. The injection volume was 3 μL. Separations were accomplished by UPLC on a Zorbax Eclipse Plus C18 column (4.6 × 100 mm, 3.5 μm particle diameter). The ESI source worked in positive ionization mode with a capillary voltage of 1 kV. The source and desolvation temperatures were set at 120 and 400 °C, respectively. The cone and desolvation gas flows were 10 and 800 L/h, respectively. UPLC-MS^2 analysis of the synthesized cotarnine and opianic acid was performed using the same analytical method and conditions applied to NSC.

2.3. Photophysical Experiments

Emission experiments were performed using a Photon Technology International (PTI) LPS-220B (steady state) and an EasyLife V (OBB) (time-resolved) fluorometers. For lifetime measurements, a diode LED (λ_{exc} = 460 nm) was used as excitation source, combined with a cut off filter (50% transmission at 475 nm), while λ_{exc} = 445 nm was employed for steady-state measurements. Experiments were performed in CH_3CN for solubility reasons. All the aerated acetonitrile solutions were prepared with absorbance <0.15 at 460 nm and 445 nm. The laser flash photolysis experiments were carried out in deaerated acetonitrile solutions, with a pulsed Nd:YAG SL404G-10 laser (Spectron Laser Systems), selecting 355 nm (12 mJ $pulse^{-1}$) as the excitation wavelength, where the absorbance of the samples was *ca.* 0.3. Further details on the system can be found in previous reports [29].

Singlet oxygen detection and quenching were performed with the same LFP equipment, but in this case a Hamamatsu NIR emission detector was used instead of the transient absorption setup. In the case of

NSC, an aerated solution of RFTA was excited at 355 nm (absorbance *ca.* 0.5), whereas in the case of Cotarnine and Opianic acid, an aerated solution of Rose Bengal with absorbance *ca.* 0.5 at 532 nm was used as a singlet oxygen generator. In both cases, power of the pulse was 10 mJ pulse^{-1}. The decay kinetics of the typical emission of $^1O_2$ ($\lambda_{max} = 1270$ nm) was recorded in aerated acetonitrile upon addition of the drugs at different concentrations.

3. Results and Discussion

3.1. Photodegradation of NSC

Photodegradation of noscapine in aerated aqueous solution was investigated in the presence of RFTA, using a solar simulator with a 420 nm filter to ensure selective light absorption by RFTA (see UV–visible spectra of NSC and RFTA, Fig. 3A and B, respectively).

The consumption of NSC and RFTA *versus* time can be observed in Fig. 4. As shown, NSC under visible light suffers total photodegradation in one hour, which is not affected by the slow photodegradation of RFTA, which remains in solution for more than two hours. The photoproducts derived from RFTA, have already been investigated in a previous work [28]. No degradation of NSC was observed in the presence of RFTA under dark condition (results not shown), whereas the abatement of NSC without RFTA by photolysis was of *ca.* 10% after 120 min.

Furthermore, the irradiated sample was submitted to LC-MS analysis, to identify the major photoproducts (see Fig. 5 and SI). The initial drug NSC gave rise to a protonated ion with *m/z* 414. The two main photoproducts afforded ions with *m/z* of 238 (photoproduct 1) and 211 (photoproduct 2), respectively, which could be associated to the two moieties of the parent drug resulting from oxidation and subsequent C—C cleavage. Moreover, loss of a water molecule in the UPLC-MS^2 analysis of the two main photoproducts resulted in detection of the corresponding dehydrated fragments with *m/z* 220 and 193, respectively. More in detail, the low intensity of the molecular ion of photoproduct 1 with *m/z* of 238 in the UPLC-MS chromatogram could be associated to the high stability of the dehydrated ion. This hypothesis was demonstrated by the UPLC-MS^2 analysis of cotarnine (*m/z* 238) independently prepared from the chemical oxidation of NSC and injected as standard (see Figs. S1-S5 in the SI) [26]. Moreover, photoproduct 2 represents a mixture of two tautomers [16], which are in equilibrium in solution. The presence of the two tautomers was confirmed by ^{1}H and ^{13}C NMR analysis of opianic acid (*m/z* 211), independently synthesized and injected as standard (see Figs. S6-S9 in the SI).

Therefore, the main photoproducts of NSC were identified as cotarnine and opianic acid (Fig. 6). The former is coincident with one of the main metabolites obtained in humans, whereas the latter is clearly related to meconine, the second major metabolite of NSC. This indicates that in the case of NSC, the combination of RF and visible light in the natural environment produces a biomimetic degradation, resulting in an oxidative cleavage of the C—C bond between the two benzylic positions. This result is of a high potential interest since it allows to develop and optimize new processes for pollutants removal and wastewater treatment.

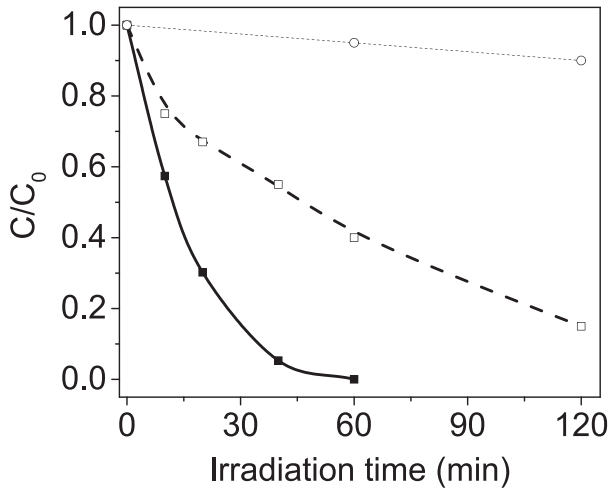

Fig. 4. Irradiation of NSC (10 ppm) in the presence of RFTA (1 ppm). Evolution of the concentration of NSC (solid line and solid square symbols) and RFTA (dashed line and empty square symbols). Control: Irradiation of NSC in the absence of RFTA (dashed line and empty circle symbol). Evolution of every reaction was analyzed by HPLC-UV (H_2O pH 9.6 / CH_3CN 45/55, *v/v*). The detection wavelength was 225 nm for NSC and 460 nm for RFTA.

3.2. The Role of the Excited Singlet State of RFTA

Fluorescence quenching measurements were performed to check the potential interaction between NSC (Fig. 7A and B) and the excited singlet photocatalyst ^{1}RFTA*. To find out which of the substructures is responsible for fluorescence quenching, analogous experiments were performed with cotarnine and opianic acid. Only in the case of cotarnine, both static and dynamic quenching were observed to a significant extent (Figs. 7C and D); their rate constants were obtained from the Stern-Volmer plots of I_0/I and τ_0/τ as a function *of* cotarnine concentration (see insets) and found to be: $k_{qS} = (1.30 \pm 0.02)x10^{10}$ M^{-1} s^{-1} and $k_{qS} = (6.1 \pm 0.9)x10^9$ M^{-1} s^{-1}, respectively. In the case of NSC and opianic acid, no reliable quenching could be proven from time-resolved experiments, while the results from the steady-state experiments (Figs. A and E) allowed determining quenching rate constant values of $k_{qS} = (3.7 \pm 0.1)x10^9$ M^{-1} s^{-1} and $k_{qS} = (2.60 \pm 0.04)x10^9$ M^{-1} s^{-1}, for NSC and opianic acid, respectively.

3.3. The Role of the Excited Triplet State of RFTA

Laser flash photolysis (LFP) was used to investigate the interaction of NSC and its substructures cotarnine and opianic acid, with the RFTA triplet excited state. The typical signal of this species (^{3}RFTA*) has a

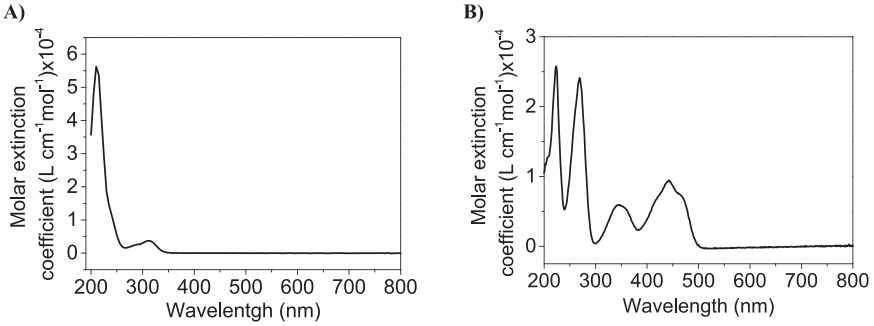

Fig. 3. UV–Vis spectra Noscapine (A) and Acetylated Riboflavin (B) in aqueous solutions.

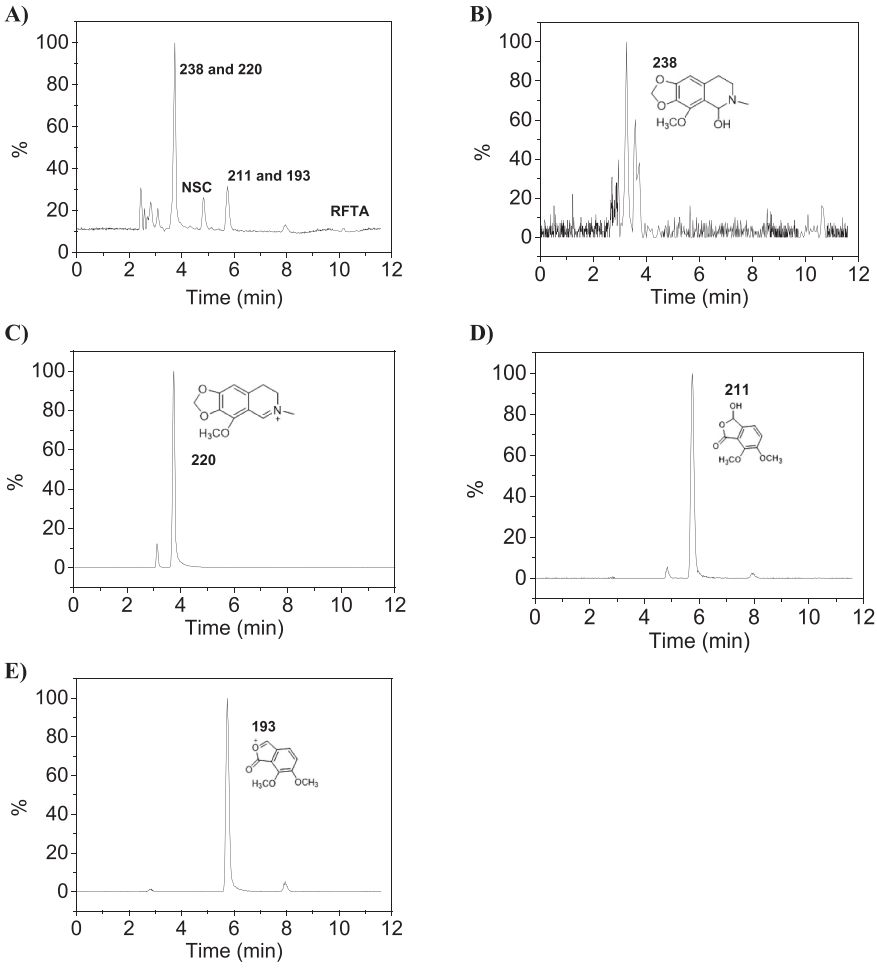

Fig. 5. A) TIC Chromatogram of the solution of NSC with RFTA after 15 min of irradiation. Selected ion monitoring (SIM) at *m/z* 238 (B), 220 (C) and corresponding dehydrated fragments 211 (D) and 193 (E).

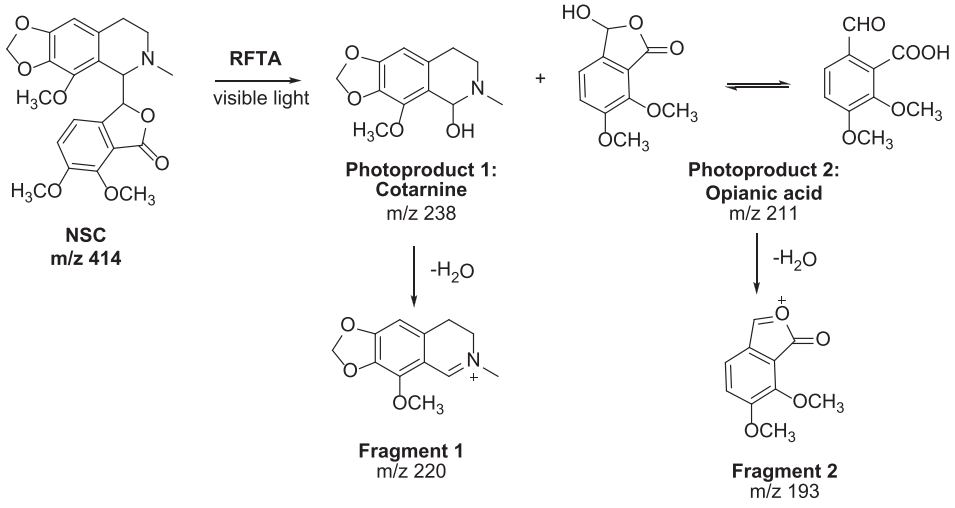

Fig. 6. RFTA-Photosensitized degradation of NSC upon exposure to visible light together with transformation products identified by UPLC-MS^2.

maximum at 380 nm and a broad absorption in the visible (from 500 to 700 nm, Fig. 8A). Interaction between NSC and ^{3}RFTA* was investigated upon recording the quenching of ^{3}RFTA* at 380 nm with progressive additions of NSC (Fig. 8B). The result of the quenching was submitted to Stern-Volmer analysis, giving rise to a quenching rate constant of (9 ± 1) x10^7 M^{-1} s^{-1}[28]. Next, similar experiments were carried out to understand the interaction between cotarnine and opianic acid with ^{3}RFTA* but changing the monitoring wavelength to 680 nm for convenience. In the case of cotarnine (Fig. 8C), quenching of ^{3}RFTA* is very efficient, the found quenching rate constant value was k_{qT} = (2.9 ±

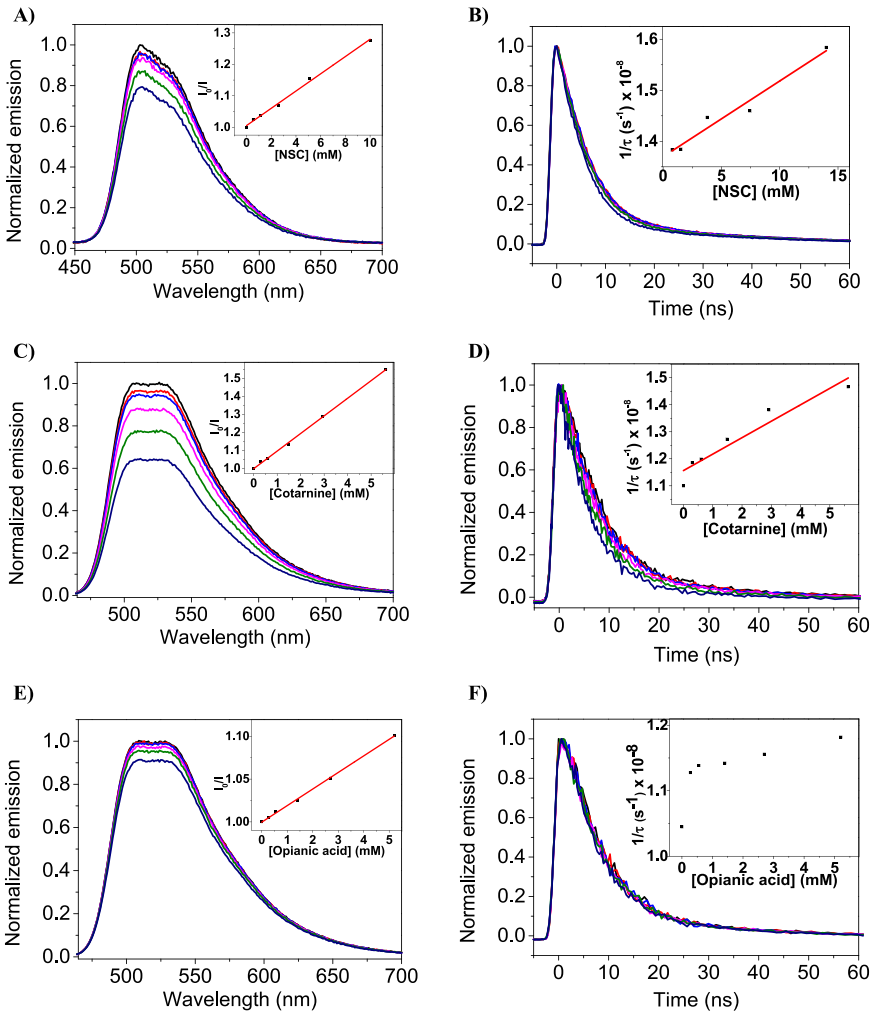

Fig. 7. Steady-state and time-resolved quenching of ^{1}RFTA* fluorescence in acetonitrile upon increasing amounts of NSC (A, B), cotarnine (C, D) and opianic acid (E, F). Insets: Stern-Volmer plots. All the measurements were carried out at room temperature in air-equilibrated CH_3CN. The excitation wavelengths were 445 nm for steady-state and 460 nm for time-resolved experiments.

0.5)x10^9 M^{-1} s^{-1} (see inset). On the contrary, the interaction between opianic acid and ^{3}RFTA* was negligible (Fig. 8D).

3.4. The Role of Singlet Oxygen

Time-resolved near infrared emission was employed for investigating the role of $^1O_2$ in the photosensitized degradation of NSC. As a matter of fact, the characteristic emission of $^1O_2$ was recorded at 1270 nm *vs* time in the presence of increasing amounts of NSC and its substructures, cotarnine and opianic acid (Fig. 9). RFTA (λ_{exc} = 355 nm) was used as $^1O_2$ generator in the case of NSC, while Rose Bengal (λ_{exc} = 532 nm) was used in the case of cotarnine and opianic acid to avoid the high absorption of the former at 355 nm. The kinetic constants were determined from the corresponding Stern-Volmer plots: k_{q1O2} = (7 ± 1)x10^5 M^{-1} s^{-1}; (4.20 ± 0.03)x10^7 M^{-1} s^{-1} and (2.6 ± 0.2)x10^6 M^{-1} s^{-1} for NSC, cotarnine and opianic acid, respectively. Again cotarnine resulted to be the most reactive compound.

3.5. Overall Discussion

In an attempt to shed light into the photodegradation mechanism of NSC mediated by RFTA and visible light, the relative contribution of the reactive species has been calculated at three potential drug concentrations in two different scenario: i) in acetonitrile, an organic solvent in which RFTA exhibits a high fluorescence quantum yield (Φ_F = 0.53), and the lifetime of the generated singlet oxygen is long (τ = 81 μs) (see data on Table 1); and ii) H_2O, in an attempt to mimic a natural environment, in which RFTA intersystem crossing is higher (Φ_{ISC} = 0.74), but lifetime of singlet oxygen is shorter (τ = 3.5 μs) (see data on Table 2). Together with NSC, also reactivity of cotarnine and opianic acid have been considered to evaluate the reactivity of the two substructures (see detailed explanation of the equations employed in the SI).

From Tables 1 and 2 we can conclude that when the concentration of NSC, cotarnine and opianic acid are as low as 10^{-8} M, dynamic quenching of the reactive species is negligible regardless its nature or the solvent media. By contrast, as the concentration increases, the ratio of quenching *vs* intrinsic decay of every reactive species increases. More in detail, in acetonitrile, in which intersystem crossing and fluorescence quantum yields are of similar values, and the lifetime of $^1O_2$ is longer than in water, the contribution of $^1O_2$ to the overall quenching is of the same order of magnitude than the quenching of ^{1}RFTA* for NSC; and even more, quenching by $^1O_2$ is the most important process in the case of opianic acid. Yet the observed quenching of the ^{3}RFTA* and $^1O_2$ by cotarnine is much higher than the observed one in the case of the other two compounds, which could be attributed to its activated benzylic position.

The situation changes in aqueous media, since quenching of the triplet excited state of RFTA plays the major role in the case of NSC and cotarnine. On the other hand, opianic acid was the less reactive one in every evaluated situation. Therefore, we could expect that

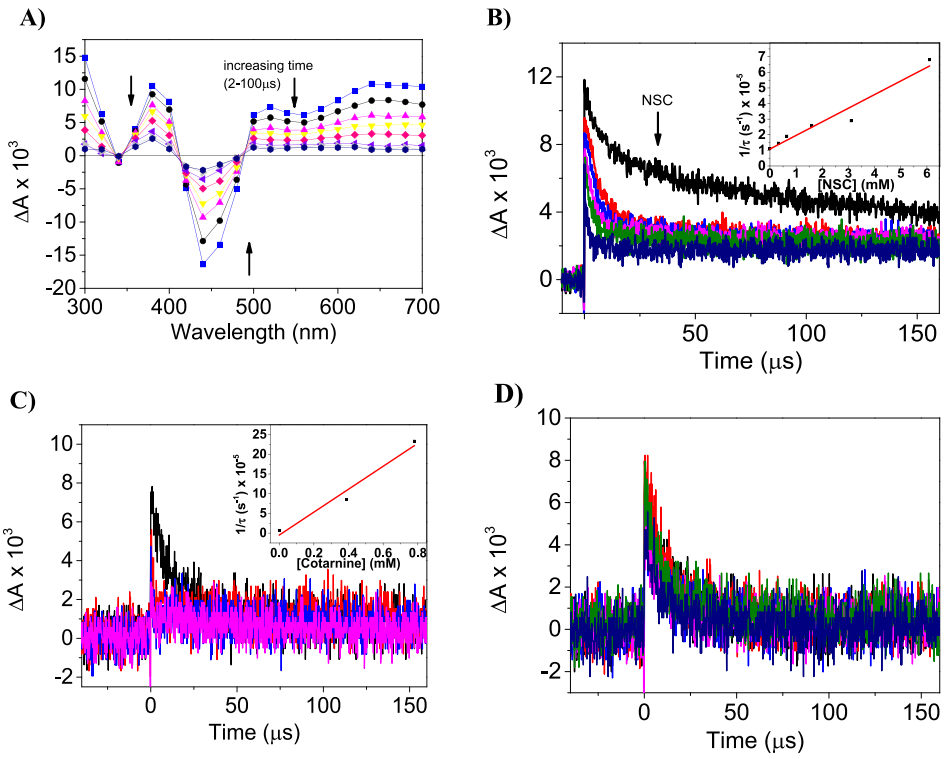

Fig. 8. A) Transient spectra recorded for RFTA at different times after the 355 nm pulse (absorbance *ca.* 0.3 at the excitation wavelength). B, C, D) Decays of ^{3}RFTA* in the presence of different concentrations of NSC (B), cotarnine (C) and opianic acid (D) at different times after the laser shot. Insets: Stern-Volmer representations. In all cases, deaerated acetonitrile was used as solvent.

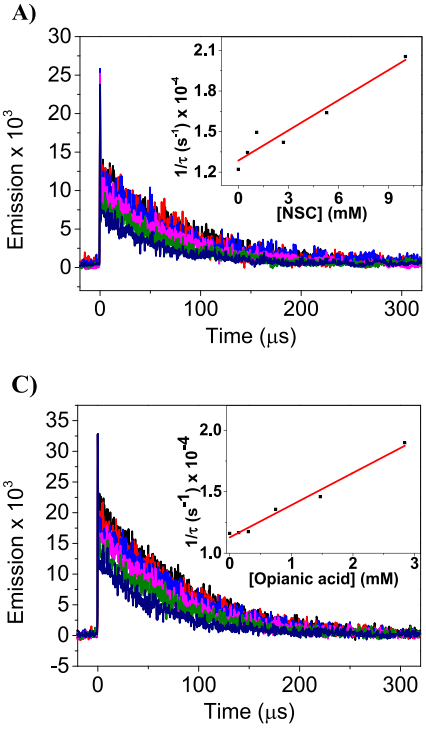

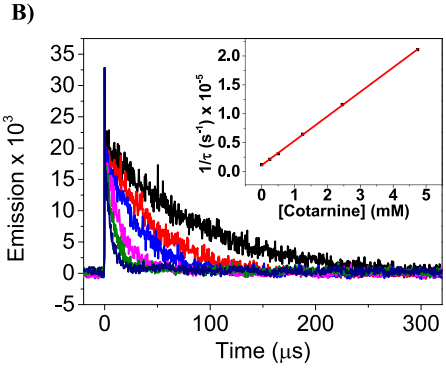

Fig. 9. Transient emission decays of $^1O_2$ monitored at 1270 nm in the presence of different amounts of noscapine (A) cotarnine (B) and opianic acid (C). Insets: Stern-Volmer analyses. In all cases, aerated acetonitrile was used as solvent. RFTA was used as a precursor for NSC experiments (λ_{exc} = 355 nm) and Rose Bengal was used as a precursor for cotarnine and opianic acid measurements (λ_{exc} = 532 nm). (For interpretation of the references to colour in this figure legend, the reader is referred to the web version of this article.)

photodegradation of NSC starts with oxidation of the tricyclic nitrogenated substructure (cotarnine-like), followed by breakage of the C—C bond between the two benzylic positions. The resulting activated benzylic position in the cotarnine photoproduct is further oxidized by electronic transfer to the ^{3}RFTA*. In fact, independent irradiation of cotarnine and opianic acid in the presence of RFTA resulted in complete photodegradation in only 60 min (see Fig. S12).

Table 1
Relative contribution of the excited singlet or triplet states of RFTA and $^1O_2$ in the quenching by NSC, cotarnine and opianic acid in acetonitrile, at selected concentrations.

[Q] (M)	Quencher	Quenching of ^{1}RFTA* (%)	^{1}RFTA* intrinsic decay (%)	Quenching of ^{3}RFTA* (%)	^{3}RFTA* intrinsic decay (%)	Quenching of ^{3}RFTA* by O_2 (%)	Quenching of $^1O_2$	$^1O_2$ intrinsic decay
10^{-3}	NSC	2.67	51.59	1.56	1.19	43.00	2.46	40.54
	Cotarnine	4.32	50.71	24.30	0.56	20.12	15.58	4.53
	Opianic acid	1.89	52.00	0.10	1.24	44.77	7.85	36.92
10^{-5}	NSC	0.03	52.99	0.02	1.27	45.70	0.03	45.67
	Cotarnine	0.05	52.98	0.55	1.25	45.18	1.50	43.68
	Opianic acid	0.02	52.99	0.00	1.27	45.72	0.10	45.62
10^{-8}	NSC	0.00	53.00	0.00	1.27	45.73	0.00	45.73
	Cotarnine	0.00	53.00	0.00	1.27	45.73	0.00	45.73
	Opianic acid	0.00	53.00	0.00	1.27	45.73	0.00	45.73

Table 2
Relative contribution of the excited singlet or triplet states of RFTA and $^1O_2$ in the quenching by NSC, cotarnine and opianic acid in water, at the selected concentrations.

[Q] (M)	Quencher	Quenching of ^{1}RFTA* (%)	^{1}RFTA* intrinsic decay (%)	Quenching of ^{3}RFTA* (%)	^{3}RFTA* intrinsic decay (%)	Quenching of ^{3}RFTA* by O_2 (%)	Quenching of $^1O_2$	$^1O_2$ intrinsic decay
10^{-3}	NSC	1.82	25.53	17.07	13.08	42.50	0.11	42.39
	Cotarnine	2.96	25.23	65.42	1.50	4.89	0.63	4.26
	Opianic acid	1.28	25.67	1.32	16.88	54.85	0.49	54.36
10^{-5}	NSC	0.02	26.00	0.23	17.36	56.40	0.00	56.40
	Cotarnine	0.03	25.99	6.87	15.79	51.31	0.08	51.24
	Opianic acid	0.01	26.00	0.01	17.41	56.57	0.01	56.56
10^{-8}	NSC	0.00	26.00	0.00	17.42	56.58	0.00	56.58
	Cotarnine	0.00	26.00	0.01	17.42	56.58	0.00	56.58
	Opianic acid	0.00	26.00	0.00	17.42	56.58	0.00	56.58

4. Conclusion

The photodegradation of the drug NSC has been achieved in less than one hour, in the presence of catalytic amount of RFTA, a derivative of the natural dye, under visible light. Analysis of the photoproducts by UPLC-MS^2, in comparison with the standards independently synthesized by chemical oxidation, allowed determining the main photodegradation pathway. The oxidative cleavage photoinduced by RFTA gives rise to the main natural metabolite cotarnine and to opianic acid, a derivative of meconine. Photophysical experiments demonstrated that this oxidative cleavage is mediated mainly by singlet oxygen in a medium in which the lifetime of $^1O_2$ is long enough or by electron transfer to RFTA in its excited triplet state if the photodegradation happens in aqueous media, in which the lifetime of $^1O_2$ is very short. The investigation of the role played by the radical species, identified in this work, allows the optimization of the experimental conditions required to develop effective new bio-inspired removal processes by using the non-toxic photosensitizer RFTA.

CRediT authorship contribution statement

Alice Pavanello: Investigation, Methodology, Data curation, Writing – original draft. **Debora Fabbri:** Investigation, Methodology, Data curation. **Paola Calza:** Conceptualization, Supervision, Project administration, Funding acquisition. **Debora Battiston:** Investigation, Methodology, Data curation. **Miguel A. Miranda:** Conceptualization, Supervision, Funding acquisition, Writing – review & editing. **M. Luisa Marin:** Conceptualization, Supervision, Project administration, Funding acquisition, Writing – review & editing.

Declaration of Competing Interest

The authors declare no conflict of interest.

Acknowledgments

This work has been partially funded by the European Union, under the Marie Skłodowska-Curie scheme (Grant No 765860, AQUAlity). The Generalitat Valenciana (PROMETEO/2017/075) and the Spanish Government (Grant PID2019-110441RB-C33 financed by MCIN/AEI/10.13039/501100011033) are also gratefully acknowledged.

Appendix A. Supplementary data

Supplementary data to this article can be found online at https://doi.org/10.1016/j.jphotobiol.2022.112415.

References

[1] S. Klemenc, Noscapine as an adulterant in illicit heroin samples, Forensic Sci. Int. 108 (2000) 45–49, https://doi.org/10.1016/S0379-0738(99)00201-7.
[2] A.C.G. Rida, Padmashree; LiVecche, Dillon; Ogden, Angela; Zhou, Jun; Ritu, the noscapine chronicle: a pharmaco-historic biography of the opiate alkaloid family and its clinical applications, Physiol. Behav. 35 (2015) 1072–1096, https://doi.org/10.1002/med.21357.The.
[3] M.A. Altinoz, G. Topcu, A. Hacimuftuoglu, A. Ozpinar, A. Ozpinar, E. Hacker, İ. Elmaci, Noscapine, a non-addictive opioid and microtubule-inhibitor in potential treatment of glioblastoma, Neurochem. Res. 44 (2019) 1796–1806, https://doi.org/10.1007/s11064-019-02837-x.
[4] H.A. Bickerman, A.L. Barach, The experimental production of cough in human subjects induced by citric acid aerosols; preliminary studies on the evaluation of antitussive agents, Am J Med Sci 228 (1954) 156–163, https://doi.org/10.1097/00000441-195408000-00005.

[5] D.W. Empey, L.A. Laitinen, G.A. Young, C.E. Bye, D.T.D. Hughes, Comparison of the antitussive effects of codeine phosphate 20 mg, dextromethorphan 30 mg and noscapine 30 mg using citric acid-induced cough in normal subjects, Eur. J. Clin. Pharmacol. 16 (1979) 393–397, https://doi.org/10.1007/BF00568199.
[6] B. Sung, K.S. Ahn, B.B. Aggarwal, Noscapine, a benzylisoquinoline alkaloid, sensitizes leukemic cells to chemotherapeutic agents and cytokines by modulating the NF-κB signaling pathway, Cancer Res. 70 (2010) 3259–3268, https://doi.org/10.1158/0008-5472.CAN-09-4230.
[7] K. Ye, Y. Ke, N. Keshava, J. Shanks, J.A. Kapp, R.R. Tekmal, J. Petros, H.C. Joshi, Opium alkaloid noscapine is an antitumor agent that arrests metaphase and induces apoptosis in dividing cells, Proc. Natl. Acad. Sci. U. S. A. 95 (1998) 1601–1606, https://doi.org/10.1073/pnas.95.4.1601.
[8] P.E. Ghaly, C.D.M. Churchill, R.M. Abou El-Magd, Z. Hájková, P. Dráber, F.G. West, J.A. Tuszynski, Synthesis and biological evaluation of structurally simplified noscapine analogues as microtubule binding agents, Can. J. Chem. 95 (2017) 649–655, https://doi.org/10.1139/cjc-2016-0649.
[9] N. Kumar, D. Sood, P.J. van der Spek, H.S. Sharma, R. Chandra, Molecular binding mechanism and pharmacology comparative analysis of noscapine for repurposing against SARS-CoV-2 protease, J. Proteome Res. (2020), https://doi.org/10.1021/acs.jproteome.0c00367.
[10] N. Kumar, A. Awasthi, A. Kumari, D. Sood, P. Jain, T. Singh, N. Sharma, A. Grover, R. Chandra, Antitussive noscapine and antiviral drug conjugates as arsenal against COVID-19: a comprehensive chemoinformatics analysis, J. Biomol. Struct. Dyn. 0 (2020) 1–16, https://doi.org/10.1080/07391102.2020.1808072.
[11] National Institute of Technology and Evaluation, Japan CHEmicals Collaborative Knowledge database (J-CHECK). https://www.nite.go.jp/chem/jcheck/List6Action?category=211&request_locale=en, 2021.
[12] S.A. Ebrahimi, Noscapine, a possible drug candidate for attenuation of cytokine release associated with SARS-CoV-2, Drug Dev. Res. (2020), https://doi.org/10.1002/ddr.21676.
[13] J. Kamei, Role of opioidergic and serotonergic mechanisms in cough and antitussives, Pulm. Pharmacol. 9 (1996) 349–356, https://doi.org/10.1006/pulp.1996.0046.
[14] Y. Ke, K. Ye, H.E. Grossniklaus, D.R. Archer, H.C. Joshi, J.A. Kapp, Noscapine inhibits tumor growth with little toxicity to normal tissues or inhibition of immune responses, Cancer Immunol. Immunother. 49 (2000) 217–225, https://doi.org/10.1007/s002620000109.
[15] M.O. Karlsson, B. Dahlström, S.Å. Eckernäs, M. Johansson, A. Tufvesson Alm, Pharmacokinetics of oral noscapine, Eur. J. Clin. Pharmacol. 39 (1990) 275–279, https://doi.org/10.1007/BF00315110.
[16] N. Tsunoda, H. Yoshimura, Metabolic fate of noscapine. II. Isolation and identification of novel metabolites produced by c - c bond cleavage, Xenobiotica. 9 (1979) 181–187, https://doi.org/10.3109/00498257909038719.
[17] A. DeBono, B. Capuano, P.J. Scammells, Progress toward the development of noscapine and derivatives as anticancer agents, J. Med. Chem. 58 (2015) 5699–5727, https://doi.org/10.1021/jm501180v.
[18] P.F. Heelis, The photophysical and photochemical properties of flavins (isoalloxazines), Chem. Soc. Rev. 11 (1982) 15–39, https://doi.org/10.1039/CS9821100015.
[19] R.A. Larson, P.L. Stackhouse, T.O. Crowley, Riboflavin tetraacetate: a potentially useful photosensitizing agent for the treatment of contaminated waters, Environ. Sci. Technol. 26 (1992) 1792–1798, https://doi.org/10.1021/es00033a013.
[20] M.L. Marin, L. Santos-Juanes, A. Arques, A.M. Amat, M.A. Miranda, Organic photocatalysts for the oxidation of pollutants and model compounds, Chem. Rev. 112 (2012) 1710–1750, https://doi.org/10.1021/cr2000543.
[21] A. Pajares, J. Gianotti, G. Stettler, S. Bertolotti, S. Criado, A. Posadaz, F. Amat-Guerri, N.A. García, Modelling the natural photodegradation of water contaminants: a kinetic study on the light-induced aerobic interactions between riboflavin and 4-hydroxypyridine, J. Photochem. Photobiol. A Chem. 139 (2001) 199–204, https://doi.org/10.1016/S1010-6030(00)00416-0.
[22] E. Reynoso, M.B. Spesia, N.A. García, M.A. Biasutti, S. Criado, Riboflavin-sensitized photooxidation of ceftriaxone and cefotaxime. Kinetic study and effect on Staphylococcus aureus, J. Photochem. Photobiol. B Biol. 142 (2015) 35–42, https://doi.org/10.1016/j.jphotobiol.2014.11.004.
[23] A. Pajares, M. Bregliani, J. Natera, S. Criado, S. Miskoski, J.P. Escalada, N. A. García, Mechanism of the photosensitizing action of a mixture humic acid-riboflavin in the degradation of water-contaminants, J. Photochem. Photobiol. A Chem. 219 (2011) 84–89, https://doi.org/10.1016/j.jphotochem.2011.01.021.
[24] O. Cabezuelo, R. Martinez-Haya, N. Montes, F. Bosca, M.L. Marin, Heterogeneous riboflavin-based photocatalyst for pollutant oxidation through electron transfer processes, Appl. Catal. B Environ. 298 (2021), 120497, https://doi.org/10.1016/j.apcatb.2021.120497.
[25] D.U. Mccormick, Flavin derivatives via bromination of the 8-methyl substituent (1), J. Heterocyclic Chem. 7 (1970) 447–450, https://doi.org/10.1002/jhet.5570070240C.
[26] S.K. Choudhury, P. Rout, B.B. Parida, J.C. Florent, L. Johannes, G. Phaomei, E. Bertounesque, L. Rout, Metal-free activation of C(sp3)–H bond, and a practical and rapid synthesis of privileged 1-substituted 1,2,3,4-tetrahydroisoquinolines, Eur. J. Org. Chem. 2017 (2017) 5275–5292, https://doi.org/10.1002/ejoc.201700471.
[27] N.P.F. Gonçalves, L. Iezzi, M.H. Belay, V. Dulio, N. Alygizakis, F. Dal Bello, C. Medana, P. Calza, Elucidation of the photoinduced transformations of Aliskiren in river water using liquid chromatography high-resolution mass spectrometry, Sci. Total Environ. 800 (2021), 149547, https://doi.org/10.1016/j.scitotenv.2021.149547.
[28] A. Pavanello, D. Fabbri, P. Calza, D. Battiston, M.A. Miranda, M.L. Marin, Photocatalytic degradation of drugs in water mediated by acetylated riboflavin and visible light: a mechanistic study, J. Photochem. Photobiol. B Biol. 221 (2021), 112250, https://doi.org/10.1016/j.jphotobiol.2021.112250.
[29] R. Martinez-Haya, J. Gomis, A. Arques, A.M. Amat, M.A. Miranda, M.L. Marin, Direct detection of the triphenylpyrylium-derived short-lived intermediates in the photocatalyzed degradation of acetaminophen, acetamiprid, caffeine and carbamazepine, J. Hazard. Mater. 356 (2018) 91–97, https://doi.org/10.1016/j.jhazmat.2018.05.023.